Progress In Electromagnetics Research Letters, Vol. 1, 263–273, 2008

TUNNEL DIODE INTEGRATED E-SHAPED PATCH ANTENNA FOR BROADBAND OPERATION

J. A. Ansari and R. B. Ram

Department of Electronics and Communication
University of Allahabad
Allahabad-211002, India

Abstract—A tunnel diode integrated E-shaped patch antenna is proposed and analyzed using equivalent circuit concept. It is found that bias voltage of tunnel diode controls the performance of the antenna. Various tunable frequency bands are obtained by selecting suitable bias voltage while antenna topology remains unchanged. Bandwidth of the tunnel diode integrated patch improves to 40.26% over the 32.58% bandwidth of the patch. The radiation pattern also varies with bias voltage and a considerable improvement in beamwidth is observed however radiated power remains almost same.

1. INTRODUCTION

The microstrip antenna is very popular in wireless and satellite communications that require wide bandwidth to accommodate the large amount of data to be transmitted within a short period of time. However, in practice, the microstrip antenna suffers from inherent narrow bandwidth that restricts its wide applications. Several methods have been proposed in the past literature to widen the bandwidth of the patch antenna [1–5]. It is well known that the use of parasitic elements either in the same layer (coplanar geometry) [1] or in another layer (stacked geometry) [2] is a very useful method for improving the bandwidth. But the coplanar geometry has disadvantage of increasing lateral size and stacked geometry has disadvantage of increasing the thickness of the antenna. Therefore, there has been a great demand of single-layer single-patch antenna for the broadband operation. In 1995, Huynh and Lee [3] suggested a single-layer single patch antenna using U-slot and reported that 10–40% impedance bandwidth could be achieved without adding parasitic elements to the patch. In 2001, Yang et al. [4] reported that the impedance bandwidth of the antenna

could be increased above 30% by incorporating slots into one of radiating edges of the rectangular patch resulting into E-shaped patch. In 2007, Ang and Chung [5] have designed a wide band E-shaped microstrip antenna for high-speed wireless local area networks (IEEE 802.11a standard) and other wireless communication systems covering frequency band of 675 MHz ranging from 5.15 GHz to 5.825 GHz.

It may be mentioned that the integration of one or more active devices with the patch could be used to further increase the bandwidth of a single-layer single patch antenna [6]. The other advantage of using tunnel diode is its low voltage requirements (110–550 mV), very wide temperature range (−73°C to 150°C) of operation and extremely high speed of operation (5–80 mA/pF) [6]. Therefore, in the present paper, a tunnel diode integrated E-shaped patch antenna is presented to further widen the bandwidth of E-shaped patch antenna (ESPA). The details of investigations are given in the following sections.

2. ANTENNA DESIGN AND FORMULATION

The geometrical configuration of the tunnel diode integrated E-shaped patch antenna is shown in Figs. 1(a) & (b). The microstrip patch is fed using a 50 ohm coaxial probe with the inner diameter of 0.127 cm. E-shaped patch antenna is considered as a rectangular patch of length $L_P = 50$ mm and width $W_P = 70$ mm with two parallel notches of length $L_n = 40$ mm and width $W_n = 6$ mm introduced at one of its radiating edges. The two notches are positioned ($P_n = 10$ mm) symmetrically with respect to the feed point $y_0 = 10$ mm. The thickness of air substrate material ($\varepsilon_r = 1.0$) between the patch and the ground plane is $h = 15$ mm.

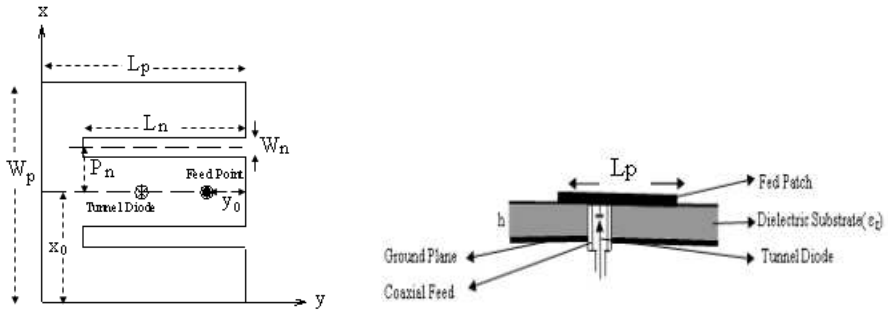

(a) Top view (b) Side view

Figure 1. Geometry of tunnel diode integrated ESPA.

It may be considered that E-shaped patch is consisted of three rectangular wings. One wing is located in the center and resistance R_1, inductance L_1 and capacitance C_1 characterize it. Another two identical wings are situated at two sides of the center wing and these are separated from the center wing by identical notches of width W_n. Resistance R_2, inductance L_2 and capacitance C_2 are the circuit parameters of each of two side wings. The parameters R_1, R_2, L_1 and C_1 are calculated using modal expansion cavity model [7]. The inductance L_2 and capacitance C_2 of the side wing are obtained by adding additional notch capacitance ΔC and notch inductance ΔL in series to the inductance L_1 and capacitance C_1 [4]. Therefore, L_2 and C_2 are given as

$$L_2 = L_1 + \Delta L \tag{1}$$

and

$$C_2 = \frac{C_1 \times \Delta C}{C_1 + \Delta C} \tag{2}$$

The notch inductanceΔL and notch capacitance ΔC are calculated as [8] and [9] respectively.

A common rectangular patch is represented by a parallel combination of resistance, inductance and capacitance [7]. Therefore, the equivalent circuit of the center wing and side wing are given as shown in Figs. 2(a) & (b). From Fig. 2(a), the impedance Z_{CW} of center wing can be derived as

$$Z_{CW} = \frac{1}{\frac{1}{R_1} + j\omega C_1 + \frac{1}{j\omega L_1}} \tag{3}$$

From the simplified equivalent circuit of side wing, shown in Fig. 2(c), its impedance Z_{SW} can be derived as

$$Z_{SW} = \frac{1}{\frac{1}{R_2} + j\omega C_2 + \frac{1}{j\omega L_2}} \tag{4}$$

Thus E-shaped patch has two resonators having distinguishable resonance frequencies. These two resonators couple each other and provide broadband characteristics to the antenna. The equivalent circuit of the E-shaped patch is shown in Fig. 2(d); from which its impedance can be derived as

$$Z_{ESPA} = \frac{(Z_{CW} + j\omega C_c)\, Z_{SW}}{Z_{CW} + Z_{SW} + j\omega C_c} \tag{5}$$

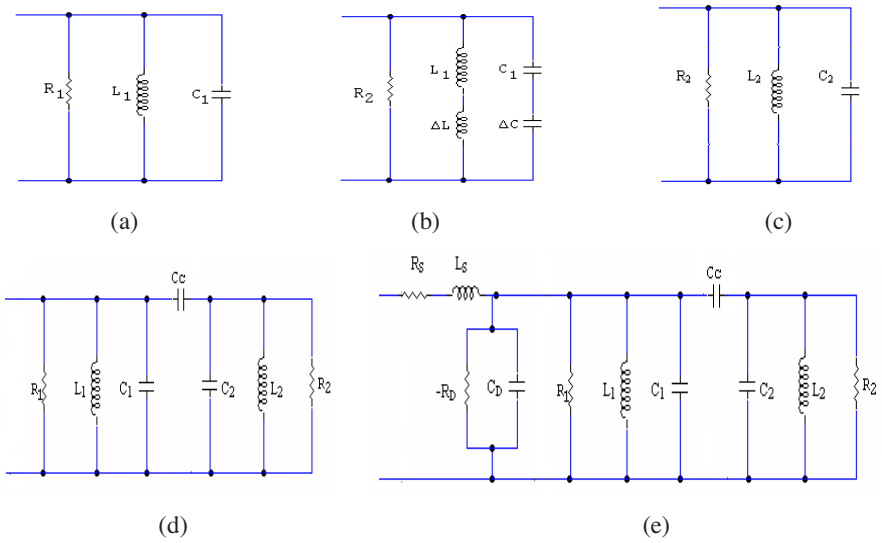

Figure 2. Equivalent circuit of (a) center wing, (b) side wing, (c) side wing (simplified), (d) E-shaped patch antenna, and (e) proposed antenna.

Table 1. Specifications of the tunnel diode.

Type	Ga-As
Series resistance (R_S)	1.0 ohm
Series inductance (L_S)	6.7500 nH
Negative resistance (R_D)	-125 ohm
Self resonance frequency (f_S)	1.0282 GHz
Resistive cut-off frequency (f_R)	4.6544 GHz
Charge concentration (N)	$6.45 \times 10^{19}\,\mathrm{cm}^{-3}$
Junction area (A)	$1.025 \times 10^{-6}\,\mathrm{cm}^2$
Bias voltage (V)	110–550 mV

The equivalent circuit for a tunnel diode (specifications are given in the Table 1) consists of resistance R_S and inductance L_S in series and the negative resistance R_D and junction capacitance C_D in parallel [10]. Therefore, when a tunnel diode is integrated to the patch the resonance feature of ESPA is changed to further increase the bandwidth. The

placement of the diode is so chosen that the device impedance (Z) be matched to the input impedance (Z_{in}) of the patch. Therefore, the position (y) of the diode from the radiating edge of the patch is given as

$$y = \frac{L_P}{\pi} \cos^{-1} \sqrt{\frac{Z}{Z_{in}}} \tag{6}$$

The equivalent circuit of tunnel diode integrated ESPA is shown in Fig. 2(e). From this figure, the input impedance of the tunnel diode integrated ESPA can be derived as

$$Z_{in} = Z_S + \frac{Z_D Z_{ESPA}}{Z_D + Z_{ESPA}} \tag{7}$$

where

$$Z_S = R_S + j\omega L_S \tag{8}$$

and

$$Z_D = \frac{1}{\frac{1}{-R_D} + j\omega C_D} \tag{9}$$

The return loss (RL) for the antenna is given as

$$RL = 20 \log_{10} |\Gamma|, \quad \Gamma = (Z_{in} - Z_0)/(Z_{in} + Z_0) \tag{10}$$

in which Z_0 is the characteristic impedance of the feeding line (50 ohm).

The operating frequency of a tunnel diode oscillator circuit is given by [10]

$$\mathrm{Im}[Y] = 0. \tag{11}$$

where Y is the admittance of the circuit as seen by the negative resistance $-R_D$. For the circuit shown in the Fig. 2(e), the value of Im$[Y]$ can be derived as

$$\mathrm{Im}[Y] = \frac{\begin{pmatrix} \big[L_e \left(R_S R_e - \omega^2 R_S R_e L_e (C_e + C_D)\right) - \omega^2 L_e L_S \\ +(R_e - \omega^2 R_e L_e (C_e + C_D)) \\ (R_S L_e + R_e L_S - \omega^2 R_e L_e L_S (C_e + C_D))\big] \end{pmatrix}}{\begin{pmatrix} \left(R_S R_e - \omega^2 R_S R_e L_e (C_e + C_D) - \omega^2 R_e L_e L_S\right)^2 \\ +(R_S L_e + R_e L_S - \omega^2 R_e L_e L_S (C_e + C_D) + R_e L_e)^2 \end{pmatrix}} \tag{12}$$

here $R_e = \frac{R_1 R_2}{R_1 + R_2}$, $L_e = \frac{L_1 L_2}{L_1 + L_2}$ and $C_e = \frac{(C_1 + C_2) Cc}{C_1 + C_2 + Cc}$.

Therefore, from Equations (11) & (12), one can get

$$\omega^4 R_e^2 L_e^2 (C_e+C_D)^2 - \omega^2 (R_S R_e L_e^2 (C_e+C_D) + L_e^2 L_S + 2R_e^2 L_e L_S (C_e+C_D) + R_e^2 L_e^2 (C_e+C_D)) + 2R_S R_e L_e + R_e^2 (L_S + L_e) = 0 \quad (13)$$

This equation can be solved for the operating frequency f_0 given as

$$f_0 = \frac{1}{2\pi} \left[\frac{(C_e+C_D)(2R_S R_e L_e + 2R_e^2 L_e L_S + R_e^2 L_e^2) + L_e^2 L_S \pm \left[\{(C_e+C_D)(2R_S R_e L_e^2 + 2R_e^2 L_e L_S + R_e^2 L_e) + L_e L_S\}^2 - 4R_e^2 L_e^2 L_S (C_e+C_D)^2 (2R_s R_e L_e + R_e^2 (L_s+L_e)) \right]^{1/2}}{2R_e^2 L_e^2 L_S (C_e+C_D)^2} \right]^{1/2} \quad (14)$$

The radiation patterns of ESPA and the proposed antenna can be calculated with approximation of E-shaped patch as a rectangular patch [11]

$$E(\phi) = \frac{jk_0 W_P V e^{-jk_0 r}}{\pi r} \cos(kh\cos\theta) \left[\frac{\sin\left(\frac{k_0 W_P}{2}\sin\phi\sin\theta\right)}{\frac{k_0 W_P}{2}\sin\phi\sin\theta} \right] \cos\left(\frac{k_0 L_P}{2}\sin\theta\sin\phi\right)\cos\phi \quad (15)$$

where $0 \le \phi \le \dfrac{\pi}{2}$

$$E(\theta) = -\frac{jk_0 W_P V e^{-jk_0 r}}{\pi r} \cos(kh\cos\theta) \left[\frac{\sin\left(\frac{k_0 W_P}{2}\sin\phi\sin\theta\right)}{\frac{k_0 W_P}{2}\sin\phi\sin\theta} \right] \cos\left(\frac{k_0 L_P}{2}\sin\theta\sin\phi\right)\cos\theta\sin\phi \quad (16)$$

where $0 \le \theta \le \dfrac{\pi}{2}$

where V is radiating edge voltage, r is the distance of an arbitrary point, k and k_0 are the wave numbers in dielectric and free space media.

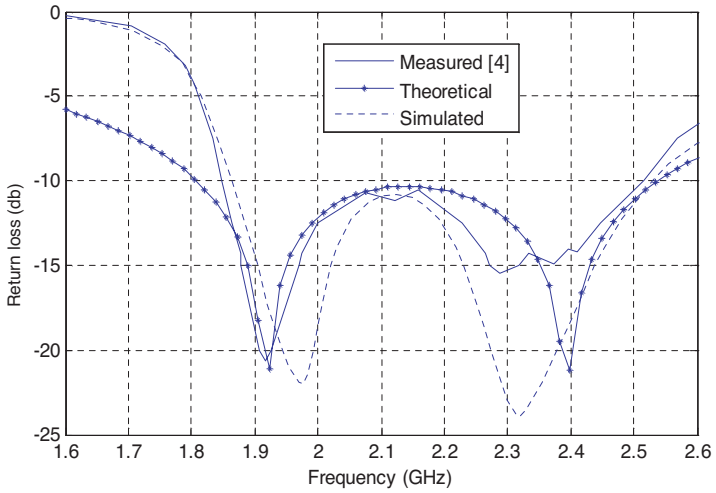

Figure 3. Variation of return loss with frequency for ESPA.

3. CALCULATIONS AND DISCUSSION OF RESULTS

Figure 3 shows the variation of return loss for ESPA as a function of frequency; for which the calculations were made using Equations (5) & (10). It is found that theoretical lower and higher resonance frequencies appear at 1.923 GHz and 2.399 GHz respectively while experimental resonance frequencies appear at 1.9 GHz and 2.4 GHz. The antenna covers a frequency band of operation from 1.821 GHz to 2.535 GHz and it shows an impedance bandwidth of 32.58% while Yang et al. have experimentally reported the 30.3% impedance bandwidth. It reveals that theoretical return loss curve is very close to the experimental [4] and the simulated (IE3D) results. The calculations for radiation pattern of ESPA were carried out using Equations (15) & (16); the resulting data are shown in Fig. 4. It depicts that the theoretical radiation patterns are identical to the experimental radiation patterns at the two resonance frequencies. Thus theoretical results together with experimental results justify the veracity of the proposed method. Further, this method is extended to analyze the performance of the proposed antenna.

The variation of return loss with frequency for the proposed antenna at different bias voltage is shown in Fig. 5; for which calculations were accomplished using Equations (7) and (10). It is observed that the proposed antenna offers a varying tunable band of frequency that varies from 806.4 MHz (bandwidth 40.26%) to

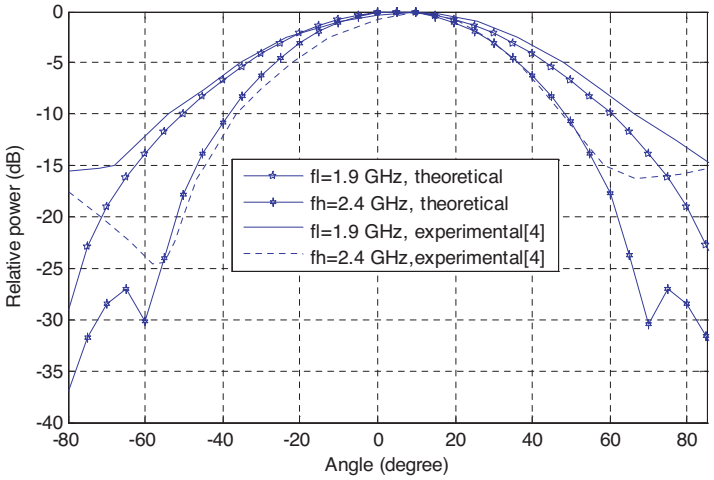

Figure 4. Radiation patterns for ESPA at lower resonance frequency (fl) and higher resonance frequency (fh).

640.8 MHz (bandwidth 33.42%) with increasing bias voltage. The proposed antenna shows enhanced bandwidth as compared to the 32.58% bandwidth of ESPA for entire range of bias voltage. It is noted that the higher resonance frequency of ESPA suffers a great shift from its original value of 2.399 GHz towards lower end of frequency as bias voltage of tunnel diode changes. It decreases from 2.205 GHz to 2.028 GHz with increasing bias voltage (Vb) from 110 mV to 550 mV. Moreover, the lower resonance is almost invariant with the bias voltage. Similar results are also corroborated from the Table 2. These variations are observed due to the great effect of bias voltage on higher resonance frequency that characterizes center wing to which tunnel diode is integrated.

The radiation patterns for the proposed antenna at different bias voltage and that of ESPA at design frequency (2.15 GHz) are shown in Fig. 6. It is observed that the 3-dB beam width of the proposed antenna varies from 86.2° to 79.0° with the bias voltage. It is highest (86.2°) at the lowest bias voltage (110 mV) and lowest (79.0°) at highest bias voltage (550 mV). The beam width of the proposed antenna is enhanced by 3° at $Vb = 550$ mV and by 10.2° at $Vb = 110$ mV as compared to 76.4° beam width of ESPA. The relative radiated power of the proposed antenna is almost same as that of ESPA.

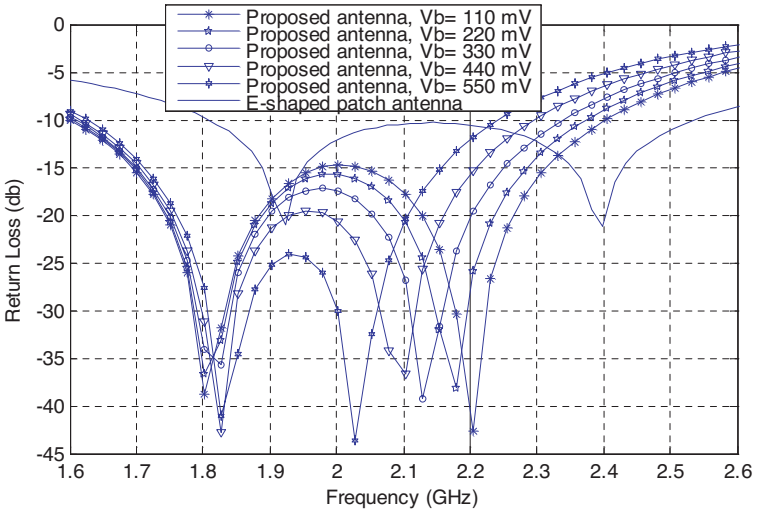

Figure 5. Variation of return loss with frequency at different bias voltage.

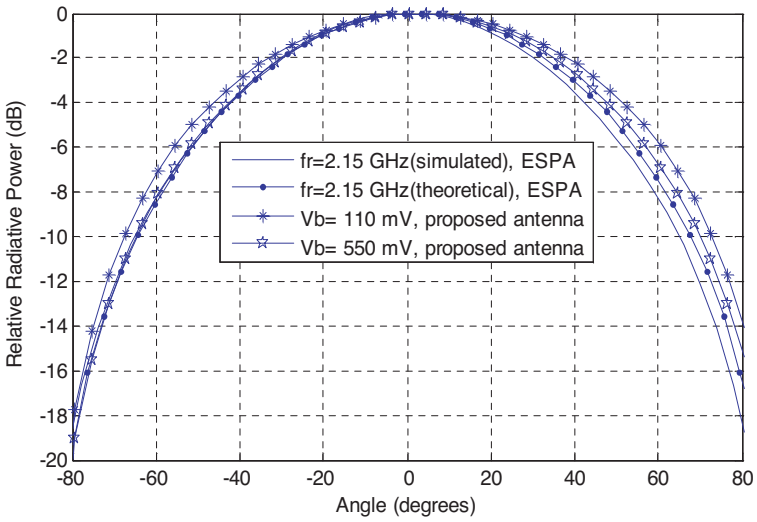

Figure 6. E-plane radiation patterns of the proposed antenna (at different bias voltage) and ESPA (at center frequency-2.15 GHz).

Table 2. Comparison of characteristics of the proposed antenna and ESPA.

	Bias Voltage (mV)	Resonance Frequency (GHz)		Frequency band (MHz)	Bandwidth (%)	Beam width (deg.)
		Lower	Higher			
For **Proposed Antenna**	110	1.802	2.205	806.4	40.26	86.2
	220	1.808	2.179	774.9	38.75	84.4
	330	1.814	2.129	718.2	36.61	82.6
	440	1.820	2.104	686.7	35.36	80.8
	550	1.827	2.028	640.8	33.42	79.0
For **ESPA**		1.923	2.399	698.4	32.58	76.4

4. CONCLUSIONS

Bias voltage of tunnel diode is an important parameter that controls not only frequency band of operation of the antenna but it also controls the beam width of the antenna. By varying the bias voltage of the diode only, the tunable band of operation can be varied from 806.4 MHz (bandwidth 40.26%) to 640.8 MHz (bandwidth 33.42%), which is applicable to modern wireless communications.

REFERENCES

1. Kumar, G. and K. C. Gupta, "Broad band microstrip antennas using additional resonators gap coupled to the radiating edges," *IEEE Trans. Antenna Propag.*, Vol. 32, No. 12, 1375–1379, Dec. 1984.
2. Nishiyama, E., M. Aikawa, and S. Egashira, "Stacked microstrip antenna for wideband and high gain," *Progress In Electromagnetics Research*, PIER 33, 29–43, 2001.
3. Huynh, T. and K. K. Lee, "Single layer single patch wideband microstrip antenna," *Electronics Letters*, Vol. 31, No. 16, 1310–1312, Aug. 1995.
4. Yang, F., X. X. Xhang, X. Ye, and Y. R. Samii, "Wide-band E-shaped patch antenna for wireless communications," *IEEE Trans. Antenna Propag.*, Vol. 49, No. 7, 1094–1100, USA, July 2001.

5. Ang, B. K. and B. K. Chung, "A wideband E-shaped microstrip patch antenna for 5–6 GHz wireless communications," *Progress In Electromagnetics Research*, PIER 75, 397–407, 2007.
6. Srivastava, S., B. R. Vishvakarma, and J. A. Ansari, "Tunnel diode loaded rectangular microstrip antenna for millimeter range," *IEEE trans. Antenna Propagate*, Vol. 51, No. 4, 750–755, April 2003.
7. Bahl, I. J. and P. Bhartia, *Microstrip Antennas*, Artech House, Dedham, MA, 1980.
8. Xhang, X. X. and F. Yang, "Study of a slit cut on a microstrip antenna and its applications," *Microwave and Optical Technology Letters*, Vol. 18, No. 4, 297–300, July 1998.
9. Bahl, I. J., *Lumped Elements for RF and Microwave Circuits*, Artech House, Boston, 2003.
10. Woo, W. F. and F. Chow, *Principles of Tunnel Diodes Circuits*, Wiely, 1964.
11. Carver, K. R. and J. W. Mink, "Microstrip antenna technology," *IEEE Trans. Antenna Propag.*, Vol. 29, No. 1, 2–23, Jan. 1981.